

REPORT DOCUMENTATION PAGE			Form Approved OMB NO. 0704-0188		
<p>The public reporting burden for this collection of information is estimated to average 1 hour per response, including the time for reviewing instructions, searching existing data sources, gathering and maintaining the data needed, and completing and reviewing the collection of information. Send comments regarding this burden estimate or any other aspect of this collection of information, including suggestions for reducing this burden, to Washington Headquarters Services, Directorate for Information Operations and Reports, 1215 Jefferson Davis Highway, Suite 1204, Arlington VA, 22202-4302. Respondents should be aware that notwithstanding any other provision of law, no person shall be subject to any penalty for failing to comply with a collection of information if it does not display a currently valid OMB control number.</p> <p>PLEASE DO NOT RETURN YOUR FORM TO THE ABOVE ADDRESS.</p>					
1. REPORT DATE (DD-MM-YYYY)		2. REPORT TYPE New Reprint		3. DATES COVERED (From - To) -	
4. TITLE AND SUBTITLE Nonequilibrium dynamics of arbitrary-range Ising models with decoherence: An exact analytic solution			5a. CONTRACT NUMBER W911NF-11-1-0400		
			5b. GRANT NUMBER		
			5c. PROGRAM ELEMENT NUMBER 611103		
6. AUTHORS Michael Foss-Feig, Kaden R. A. Hazzard, John J. Bollinger, Ana Maria Rey			5d. PROJECT NUMBER		
			5e. TASK NUMBER		
			5f. WORK UNIT NUMBER		
7. PERFORMING ORGANIZATION NAMES AND ADDRESSES Massachusetts Institute of Technology (MIT) Office of Sponsored Programs 77 Massachusetts Avenue Cambridge, MA 02139 -4307				8. PERFORMING ORGANIZATION REPORT NUMBER	
9. SPONSORING/MONITORING AGENCY NAME(S) AND ADDRESS(ES) U.S. Army Research Office P.O. Box 12211 Research Triangle Park, NC 27709-2211				10. SPONSOR/MONITOR'S ACRONYM(S) ARO	
				11. SPONSOR/MONITOR'S REPORT NUMBER(S) 59745-PH-MUR.32	
12. DISTRIBUTION AVAILABILITY STATEMENT Approved for public release; distribution is unlimited.					
13. SUPPLEMENTARY NOTES The views, opinions and/or findings contained in this report are those of the author(s) and should not be construed as an official Department of the Army position, policy or decision, unless so designated by other documentation.					
14. ABSTRACT The interplay between interactions and decoherence in many-body systems is of fundamental importance in quantum physics. In a step toward understanding this interplay, we obtain an exact analytic solution for the nonequilibrium dynamics of Ising models with arbitrary couplings (and therefore in arbitrary dimension) and subject to local Markovian decoherence. Our solution shows that decoherence significantly degrades the nonclassical correlations developed during coherent Ising spin dynamics, which relax much faster than predicted by					
15. SUBJECT TERMS Quism					
16. SECURITY CLASSIFICATION OF:			17. LIMITATION OF ABSTRACT UU	15. NUMBER OF PAGES	19a. NAME OF RESPONSIBLE PERSON Paola Cappellaro
a. REPORT UU	b. ABSTRACT UU	c. THIS PAGE UU			19b. TELEPHONE NUMBER 617-253-8137

Report Title

Nonequilibrium dynamics of arbitrary-range Ising models with decoherence: An exact analytic solution

ABSTRACT

The interplay between interactions and decoherence in many-body systems is of fundamental importance in quantum physics. In a step toward understanding this interplay, we obtain an exact analytic solution for the nonequilibrium dynamics of Ising models with arbitrary couplings (and therefore in arbitrary dimension) and subject to local Markovian decoherence. Our solution shows that decoherence significantly degrades the nonclassical correlations developed during coherent Ising spin dynamics, which relax much faster than predicted by treating decoherence and interactions separately. We also show that the competition of decoherence and interactions induces a transition from oscillatory to overdamped dynamics that is absent at the single-particle or mean-field level. These calculations are applicable to ongoing quantum information and emulation efforts using a variety of atomic, molecular, optical, and solid-state systems. In particular, we apply our results to the NIST Penning trapped-ion experiment and show that the current experiment is capable of producing entanglement amongst hundreds of quantum spins.

REPORT DOCUMENTATION PAGE (SF298)
(Continuation Sheet)

Continuation for Block 13

ARO Report Number 59745.32-PH-MUR
Nonequilibrium dynamics of arbitrary-range Ising ...

Block 13: Supplementary Note

© 2013 . Published in Physical Review A, Vol. Ed. 0 87, (4) (2013), (, (4). DoD Components reserve a royalty-free, nonexclusive and irrevocable right to reproduce, publish, or otherwise use the work for Federal purposes, and to authorize others to do so (DODGARS §32.36). The views, opinions and/or findings contained in this report are those of the author(s) and should not be construed as an official Department of the Army position, policy or decision, unless so designated by other documentation.

Approved for public release; distribution is unlimited.

Nonequilibrium dynamics of arbitrary-range Ising models with decoherence: An exact analytic solution

Michael Foss-Feig,¹ Kaden R. A. Hazzard,¹ John J. Bollinger,² and Ana Maria Rey¹

¹*JILA, NIST, and Department of Physics, University of Colorado, Boulder, Colorado 80309-0440, USA*

²*National Institute of Standards and Technology, Boulder, Colorado 80305, USA*

(Received 23 September 2012; published 3 April 2013)

The interplay between interactions and decoherence in many-body systems is of fundamental importance in quantum physics. In a step toward understanding this interplay, we obtain an exact analytic solution for the nonequilibrium dynamics of Ising models with arbitrary couplings (and therefore in arbitrary dimension) and subject to local Markovian decoherence. Our solution shows that decoherence significantly degrades the nonclassical correlations developed during coherent Ising spin dynamics, which relax much faster than predicted by treating decoherence and interactions separately. We also show that the competition of decoherence and interactions induces a transition from oscillatory to overdamped dynamics that is absent at the single-particle or mean-field level. These calculations are applicable to ongoing quantum information and emulation efforts using a variety of atomic, molecular, optical, and solid-state systems. In particular, we apply our results to the NIST Penning trapped-ion experiment and show that the current experiment is capable of producing entanglement amongst hundreds of quantum spins.

DOI: [10.1103/PhysRevA.87.042101](https://doi.org/10.1103/PhysRevA.87.042101)

PACS number(s): 03.65.Yz, 05.50.+q, 37.10.Ty, 75.10.Pq

I. INTRODUCTION

Understanding strongly correlated quantum systems in the presence of decoherence is a fundamental challenge in modern physics. While decoherence generally tends to degrade correlations, it is now widely appreciated that it can also give rise to many-body physics not possible with strictly coherent dynamics [1–3], and can be used explicitly for the creation of entanglement [4–6]. Regardless of whether one’s intention is to minimize or to harness decoherence, determining its effect on interacting many-body systems is central to quantum simulation [7], quantum information [8], and quantum metrology [9]. So far, this understanding has been hindered by the computational complexity of numerical techniques for open systems and the scarcity of exact analytic solutions. Exact solutions for dynamics of interacting quantum systems in dimensions greater than one are rare even in the absence of decoherence, and to our knowledge no such solutions have been obtained in the presence of local decoherence.

The central result of this manuscript is an exact solution, Eqs. (10)–(12), for the time dependence of all two-spin correlation functions in a system of spins interacting via arbitrary Ising couplings in any dimension, and subject to local Markovian decoherence. Our solution is applicable to a broad range of important quantum systems, including trapped ions [10–12], polar molecules [13,14], Rydberg atoms [15,16], neutral atoms in optical cavities [17,18], optical lattice clocks [19], superconducting qubits [20], quantum dots [21], and nitrogen vacancy centers [22]. Nonequilibrium dynamics in the presence of Ising interactions is highly nonclassical, and can be exploited in such systems for the generation of entanglement for use in quantum metrology and quantum information [23–28] (for instance, spin-squeezed states [23] or cluster states [29] can be produced). Here we apply our solution to trapped-ion experiments because (1) the relative importance of decoherence and coherently driven quantum correlations is controllable, (2) the tunable long-ranged interactions are generically frustrated, making

large-scale numerical simulations impractical, and (3) these experiments are the most developed, with nonequilibrium dynamics already being explored [10]. We will show that entanglement—in the metrologically useful form of spin squeezing—can be produced amongst hundreds of spins under *current* experimental conditions in Ref. [10]. We also demonstrate that expected improvements to this experiment should allow for the production of macroscopic superposition states (MSSs) in the near future.

The structure of the manuscript is as follows. In Sec. II we describe the model, which includes coherent dynamics due to arbitrary Ising interactions, and an extremely general form of Markovian decoherence including both dephasing, spin relaxation, and spin excitation. In Sec. III, we review the quantum trajectories approach to open quantum systems, which is central to our solution of the model. Section IV describes the application of quantum trajectories to computing various observables relevant to both relaxation and growth of quantum correlations. The idea is to (a) calculate these quantities exactly along a particular trajectory, and then (b) carry out the averaging over trajectories analytically. As we will show, the resulting expressions reveal that the dynamics exhibits a transition from oscillatory to overdamped behavior, an effect that is not present at the single-particle level or in a mean-field treatment of the interactions. With these solutions in hand, Sec. V considers the applications to trapped-ion experiments in general, with a particular focus on relaxation and squeezing in the recent experiment in Ref. [10]. We conclude in Sec. VI by considering several open questions and promising directions for future research.

II. MODEL

We consider far-from-equilibrium dynamics of a long-ranged Ising Hamiltonian,

$$\mathcal{H} = \frac{1}{N} \sum_{i < j} J_{ij} \hat{\sigma}_i^z \hat{\sigma}_j^z. \quad (1)$$

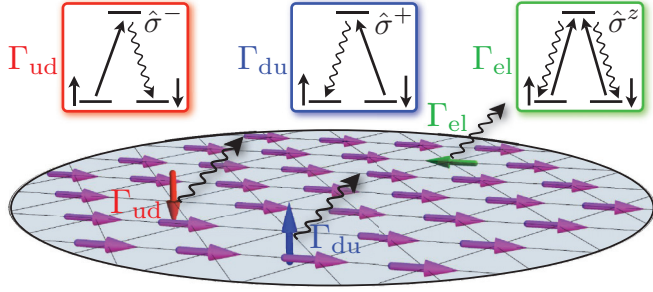


FIG. 1. (Color online) Schematic illustration of the various decoherence processes: T_1 spin relaxation with rates Γ_{ud}, Γ_{du} (red and blue spin, respectively), and T_2 dephasing with rate Γ_{el} (green spin). In atomic systems, one way this decoherence can arise is due to spontaneous emission from an excited level (top panels) [32].

Here $\hat{\sigma}^a$ ($a = x, y, z$) are Pauli matrices, \mathcal{N} is the total number of spins, and the subscripts (i, j) are site indices. Our results are valid for arbitrary J_{ij} , but given the relevance to numerous experiments we will sometimes consider power-law couplings $J_{ij} = J|\mathbf{r}_i - \mathbf{r}_j|^{-\zeta}$, where \mathbf{r}_i is the position of the i th spin in lattice units ($\zeta = 3$ for polar molecules, $\zeta = 6$ for Rydberg atoms, and $0 < \zeta < 3$ for trapped ions). In the presence of local decoherence, the most general Markovian dynamics of the system reduced density matrix obeys a master equation [30],

$$\hbar \dot{\rho} = -i(\mathcal{H}_{\text{eff}}\rho - \rho\mathcal{H}_{\text{eff}}^\dagger) + \mathcal{D}(\rho). \quad (2)$$

The effective Hamiltonian \mathcal{H}_{eff} and dissipator \mathcal{D} have contributions from all jump operators $\mathcal{J} \in \{\hat{\sigma}_j^-, \hat{\sigma}_j^+, \sqrt{\Gamma_{du}/2}, \hat{\sigma}_j^z\sqrt{\Gamma_{el}/8} : 1 \leq j \leq \mathcal{N}\}$,

$$\mathcal{H}_{\text{eff}} = \mathcal{H} - i \sum_{\text{all } \mathcal{J}} \mathcal{J}^\dagger \mathcal{J}, \quad \mathcal{D}(\rho) = 2 \sum_{\text{all } \mathcal{J}} \mathcal{J} \rho \mathcal{J}^\dagger, \quad (3)$$

where $\hat{\sigma}_j^\pm = \frac{1}{2}(\hat{\sigma}_j^x \pm i\hat{\sigma}_j^y)$. The jump operators $\hat{\sigma}_j^-, \hat{\sigma}_j^+$, and $\hat{\sigma}_j^z$ give rise to spontaneous deexcitation, spontaneous excitation, and elastic dephasing, respectively (see Fig. 1). We refer to the spin-changing processes ($\hat{\sigma}^\pm$) as Raman decoherence, and the spin-preserving processes ($\hat{\sigma}^z$) as Rayleigh decoherence. In what follows we assume an initially pure and uncorrelated density operator $\rho(0) = |\psi(0)\rangle\langle\psi(0)|$, with

$$|\psi(0)\rangle = \bigotimes_j \sum_{\sigma_j} f_j(\sigma_j) |\sigma_j\rangle. \quad (4)$$

Here $\sigma_j = \pm 1$ are the eigenvalues of $\hat{\sigma}_j^z$, $f_j(1) = \cos(\theta_j/2)e^{i\varphi_j/2}$, and $f_j(-1) = \sin(\theta_j/2)e^{-i\varphi_j/2}$, for arbitrary θ_j and φ_j .

III. QUANTUM TRAJECTORIES APPROACH

Our approach to the solution of Eq. (2) for the chosen initial conditions and arbitrary $\{\Gamma_{ud}, \Gamma_{du}, \Gamma_{el}\}$ is based on the quantum trajectories method [31], in which $|\psi(0)\rangle$ is time evolved with the effective Hamiltonian,

$$\mathcal{H}_{\text{eff}} = \mathcal{H} - \frac{i}{2} \sum_j \left(\frac{\Gamma_r}{2} + \frac{\Gamma_{el}}{4} + 2\gamma \hat{\sigma}_j^z \right), \quad (5)$$

and the dynamics are interspersed with stochastic applications of the jump operators. In Eq. (5) we have defined $\Gamma_r =$

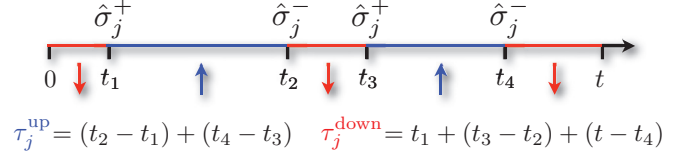


FIG. 2. (Color online) Series of Raman flips of the spin on site j can be formally accounted for as a magnetic field of strength $2J_{jk}/\mathcal{N}$ acting for a time $\tau_j^{\text{up}} - \tau_j^{\text{down}}$. In the notation defined below, this series of jumps is represented by the operator $\hat{Q}_j \propto \hat{\sigma}_j^+(t_1)\hat{\sigma}_j^-(t_2)\hat{\sigma}_j^+(t_3)\hat{\sigma}_j^-(t_4)$.

$\Gamma_{ud} + \Gamma_{du}$ and $\gamma = \frac{1}{4}(\Gamma_{ud} - \Gamma_{du})$. According to the standard prescription [31], a particular trajectory consists of a set of jump times $\{t_1, t_2, \dots\}$, which are selected by equating the norm of the wave function to a random number uniformly distributed between 0 and 1. Choosing which jump operator to apply at each time requires calculating all expectation values $\langle \mathcal{J}^\dagger \mathcal{J} \rangle$. Because \mathcal{H} is Hermitian and commutes with all products $\mathcal{J}^\dagger \mathcal{J}$, it has no effect on the selection of the jumps, which can therefore be obtained for each spin independently (since the anti-Hermitian part of \mathcal{H}_{eff} does not couple different spins). We note, however, that \mathcal{H} does not commute with the recycling term $\mathcal{D}(\rho)$ defined in Eq. (3). With the jump times and jump operators in hand, we define a string of n_j (time-labeled) jump operators on site j as $\hat{Q}_j = \mathcal{J}_j^1(t_1^1) \times \dots \times \mathcal{J}_j^{n_j}(t_j^{n_j})$. The time evolution of the wave function along a trajectory is then

$$|\psi(t)\rangle = \mathcal{T} \left(e^{-i\mathcal{H}_{\text{eff}}t} \prod_j \hat{Q}_j \right) |\psi(0)\rangle, \quad (6)$$

where the time-ordering operator \mathcal{T} enforces that the jump operators are interspersed in the time evolution according to their time labels.

The time ordering of the Rayleigh jumps can be ignored: because $[\hat{\sigma}_j^z, \mathcal{H}_{\text{eff}}] = 0$ and $[\hat{\sigma}_j^z, \hat{\sigma}_j^\pm] = \pm 2\hat{\sigma}_j^\pm$, all Rayleigh jumps can be evaluated at $t = 0$ (their commutation with Raman jumps only affects the overall sign of the wave function). To the contrary, the Raman jump operators are structurally similar to a transverse field, and do not commute with \mathcal{H}_{eff} ; their time ordering cannot be so easily accounted for. However, imagine that spin j undergoes a single Raman jump, created by applying $\hat{\sigma}_j^+$ at time t . This jump operator not only flips spin j into the up position, but also removes all parts of the wave function in which spin j pointed up immediately before time t . Hence it is as if this spin pointed down before time t , and up after time t . Since spin j is always in an eigenstate of $\hat{\sigma}_j^z$ it is a spectator to the Ising dynamics, but it does influence the other spins via the Ising coupling J_{jk} ; formally it acts on spin k as an inhomogeneous magnetic field of strength $2J_{jk}/\mathcal{N}$ that pointed down before t and up after t . For a spin on site j that undergoes multiple Raman processes, the same reasoning allows us to treat it as a field of strength $2J_{jk}/\mathcal{N}$ that acts for a time $\tau_j = (\tau_j^{\text{up}} - \tau_j^{\text{down}})$, where $\tau_j^{\text{up(down)}}$ is the total amount of time that spin j spends pointing up(down) along z (see Fig. 2). Hence we are free to evaluate all of the jump operators at $t = 0$ to give $|\tilde{\psi}\rangle = \prod_j \hat{Q}_j |\psi\rangle$, thus ignoring the time ordering in Eq. (6), so long as we evolve

$|\tilde{\psi}\rangle$ with a modified time-evolution operator

$$\mathcal{U} = \exp \left[-it \left(\mathcal{H}' + \sum_j (\eta_j - i\gamma) \hat{\sigma}_j^z \right) \right]. \quad (7)$$

Here $\eta_j = \frac{1}{N_t} \sum_k J_{jk} \tau_k$ accounts for the magnetic field of all Raman-flipped ions, \mathcal{H}' is obtained from \mathcal{H} by ignoring the spin-spin couplings to spins that have undergone Raman jumps, and γ accounts for the non-Hermitian part of \mathcal{H}_{eff} that is *not* proportional to the identity operator.

The expectation value of an arbitrary operator \hat{O} at the end of a particular quantum trajectory is therefore given by $\langle \hat{O} \rangle = \langle \tilde{\psi} | \mathcal{U}^\dagger \hat{O} \mathcal{U} | \tilde{\psi} \rangle / \langle \tilde{\psi} | \mathcal{U}^\dagger \mathcal{U} | \tilde{\psi} \rangle$, and formally taking the average over all trajectories (denoted by an overbar) we have $\text{tr}[\rho \hat{O}] = \langle \hat{O} \rangle$. Along with Eq. (7), these constitute a formal solution for the dynamics of any observable. We now proceed to derive closed-form expressions for the transverse spin-length and spin-spin correlation functions—which have not been derived previously even in the *absence* of decoherence. These are the central result of this paper.

IV. TRANSVERSE-SPIN LENGTH AND CORRELATION FUNCTIONS

Relaxation of the transverse-spin length in an Ising-type spin model is a canonical example of equilibration in a closed quantum system [33–35]. In the present model, such relaxation occurs due to a combination of the proliferation of quantum fluctuations *and* the equilibration with the environment (decoherence). Our theoretical treatment allows for both effects to be treated simultaneously, and therefore, in principle, the disentangling of these two physically different (but sequentially similar) processes. While such relaxation does not directly indicate quantum correlations or entanglement, in the absence of decoherence it nevertheless is entirely due to the buildup of quantum correlations—at the mean-field level coherent relaxation is absent. The correlations that develop during the dynamics can be understood in more detail by looking at two-spin correlation functions—for instance, these furnish a complete description of spin squeezing [23]. In the absence of decoherence and for all-to-all coupling ($\zeta = 0$), it is well known [23] that the transverse-spin component revives at a time $\tau_r = N\pi\hbar/(2J)$, and that a highly entangled macroscopic-superposition state (MSS) appears at time $\tau_r/2$. This state is characterized by vanishing spin length but maximum transverse-spin fluctuations, and our solution can be used to assess the robustness of such fluctuations against decoherence.

To calculate the transverse-spin length along a particular trajectory, we assign the discrete-valued variables \mathcal{R}_j and \mathcal{F}_j to each lattice site, which count the number of Raman jumps and Rayleigh jumps, respectively. As we have discussed earlier, all jump operators can be applied at $t = 0$, and therefore specifying the $\{\mathcal{R}_j, \mathcal{F}_j, \tau_j\}$ on each site fully determines transverse-spin length along that trajectory. The transverse spin component in direction φ and on site j is given simply in terms of the spin-raising operator on that site, $\langle S_j^\varphi \rangle = \cos \varphi \langle S_j^x \rangle + \sin \varphi \langle S_j^y \rangle = \text{Re}[e^{-i\varphi} \langle \hat{\sigma}_j^+ \rangle]$, and

generalizing solutions obtained in Refs. [33,36], we find

$$\langle \hat{\sigma}_j^+ \rangle = \frac{\alpha_j \beta_j \sin \theta_j e^{i\varphi_j}}{2g_j(2\gamma t)} \prod_{k \neq j} e^{\frac{2iJ_{kj}\tau_k}{N}} \frac{g_k[2\alpha_k t(\gamma - iJ_{jk}/N)]}{g_k(2\gamma t\alpha_k)}. \quad (8)$$

Here $g_j(x) = \sum_\sigma |f_j(\sigma)|^2 e^{-\sigma x}$, $\alpha_j = \delta_{\mathcal{R}_j,0}$ (δ being the Kronecker-delta symbol), $\beta_j = (-1)^{\mathcal{F}_j}$, and the details of the calculation are given in Appendix A. Defining a function $\mathcal{P}(\mathcal{R}, \mathcal{F}, \tau)$ that determines the probability distribution of these variables on a given lattice site, we have

$$\overline{\langle \hat{\sigma}_j^+ \rangle} = \sum_{\text{all } \mathcal{R}} \sum_{\text{all } \mathcal{F}} \int \dots \int \prod_k d\tau_k \mathcal{P}(\mathcal{R}_k, \mathcal{F}_k, \tau_k) \langle \hat{\sigma}_j^+ \rangle. \quad (9)$$

Equation (9) constitutes a formal solution for $\overline{\langle \hat{\sigma}_j^+ \rangle}$, and it can always be evaluated efficiently by averaging $\langle \hat{\sigma}_j^+ \rangle$ over stochastically generated trajectories. However, because the noise is uncorrelated from site to site, and accordingly the expression inside the product of Eq. (8) depends only on local stochastic variables, these sums and integrals factor into N independent sets (each over the three stochastic variables), admitting closed-form expressions. We note that, while most quantum trajectories simulations average over a finite number of stochastically selected trajectories, thus giving rise to statistical errors, our approach effectively averages over an infinite number of trajectories. Hence our solutions have no statistical approximation. We have checked for small spin systems that they produce results identical to a full numerical solution of the master equation [Eq. (2)].

At this point, to avoid unnecessary complications in the ensuing expressions, we will take our initial state to point along the x axis ($\theta = \pi/2$, $\varphi = 0$), but our results easily generalize [37]. In Appendix B we explain how to evaluate these sums and integrals, and here we simply quote the result. Defining

$$\Phi(J, t) = e^{-\lambda t} [\cos(t\sqrt{s^2 - r}) + \lambda t \text{sinc}(t\sqrt{s^2 - r})],$$

with $\lambda = \Gamma_r/2$, $s = 2i\gamma + 2J/N$, and $r = \Gamma_{\text{ud}}\Gamma_{\text{du}}$, we find

$$\overline{\langle \hat{\sigma}_j^+ \rangle} = \frac{1}{2} e^{-\Gamma t} \prod_{k \neq j} \Phi(J_{jk}, t), \quad (10)$$

where the total decoherence rate is defined $\Gamma = \frac{1}{2}(\Gamma_r + \Gamma_{\text{el}})$ [38]. Similar calculations to those described above yield spin-spin correlation functions

$$\overline{\langle \hat{\sigma}_j^\mu \hat{\sigma}_k^\nu \rangle} = \frac{1}{4} e^{-2\Gamma t} \prod_{l \notin \{j, k\}} \Phi(\mu J_{jl} + \nu J_{kl}, t), \quad (11)$$

$$\overline{\langle \hat{\sigma}_j^\mu \hat{\sigma}_k^z \rangle} = \frac{1}{2} e^{-\Gamma t} \Psi(\mu J_{jk}, t) \prod_{l \notin \{j, k\}} \Phi(\mu J_{jl}, t), \quad (12)$$

with

$$\Psi(J, t) = e^{-\lambda t} (is - 2\gamma)t \text{sinc}(t\sqrt{s^2 - r}) \quad (13)$$

and $\mu, \nu = \pm$. These correlation functions, along with similar ones obtained by interchange of the site indices, completely determine the spin-spin correlations. Each instance of $\hat{\sigma}^x$ or $\hat{\sigma}^y$ in an observable generates an overall multiplicative factor of $e^{-\Gamma t}$, which would also occur if the decoherence were treated in the absence of interactions; this is the effect of decoherence at the single-particle level. The structure of $\Phi(J, t)$ captures

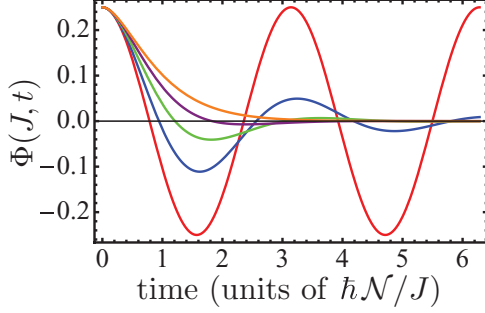


FIG. 3. (Color online) Plots of $\Phi(J, t)$ for $\gamma = 0$ and $\Gamma_r/\Gamma_r^c \in \{0, 1/4, 1/2, 3/4, 1\}$, showing a transition from oscillatory to damped behavior.

the interplay of decoherence and the many-body physics, and could not have been deduced without our exact treatment. The additional damping present in $\Phi(J, t)$ has a straightforward physical origin, which is made particularly clear by the quantum trajectories formalism. Even if a spin on site j has not undergone any quantum jumps, it experiences a fluctuating (in time and space) longitudinal magnetic field η_j due to the various other spins that have undergone quantum jumps, and thus experiences additional dephasing.

We note that for $\gamma = 0$ the function $\Phi(J, t)$ undergoes a qualitative transition from oscillatory ($s^2 > r$) to damped ($s^2 < r$) behavior when $\Gamma_r = \Gamma_r^c \equiv 4J/\mathcal{N}$ (Fig. 3). Therefore, when there is only one coupling strength J , for instance in the case of all-to-all or nearest-neighbor couplings, dynamics of the transverse-spin length and correlation functions undergoes the same transition. We note that the factors of $e^{-\Gamma t}$ in Eqs. (10)–(12) may make this transition difficult to observe experimentally, since the correlations are rapidly suppressed at the critical Γ_r^c . It is important to realize that, while such a transition is expected for a single spin in the presence of a coherence restoring drive (i.e., a transverse field), it does *not* occur for a noninteracting system in the absence of a transverse field. Hence, in the Ising model, this transition is a manifestly many-body effect, arising from the competition of decoherence and the coherent dynamics generated by the interactions. It is interesting to note that, if the Ising interaction had been treated at the mean-field level, the system would behave as a collection of independent spins undergoing decoherence and experiencing a (self-consistently determined) longitudinal field. Thus this transition cannot be captured at the mean-field level.

V. APPLICATION TO A TRAPPED-ION QUANTUM SIMULATOR

Trapped-ion systems can simulate the Hamiltonian in Eq. (1), and can accurately measure the decoherence rates Γ_{el} , Γ_{ud} , and Γ_{du} . We note that both the Born-Markov approximation and the assumption of uncorrelated decoherence processes are extremely well justified for trapped-ion systems [32]. Sample averaged spin-length and spin-spin correlation functions are easily measured in these experiments by looking at the length (and its shot-to-shot fluctuations) of various projections of the Bloch vector. In the trapped-ion experiments discussed in Ref. [10], when $\zeta = 0$ the time scale at which

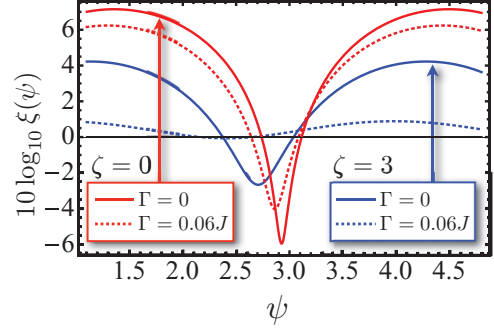


FIG. 4. (Color online) (a) Example of how spin squeezing is affected by decoherence (dashed lines are $\Gamma = 0.06J$; solid lines are for $\Gamma = 0$) for long-ranged (red, $\zeta = 0$) and short-ranged (blue, $\zeta = 3$) interactions.

quantum correlations become important for these observables, τ_c , scales with some power of the ion number: $\tau_c \sim \mathcal{N}^{1/3}$ for spin squeezing, $\sim \mathcal{N}^{1/2}$ for transverse-spin relaxation, and $\sim \mathcal{N}$ for the creation of MSS's. Taking $\mathcal{N} = 100$ and $\Gamma = 0.06J$, as is typical in that experiment, we expect the proper incorporation of decoherence to be quantitatively important even for spin squeezing, despite it being a relatively short-time indication of entanglement.

Equations (11) and (12) allows us to exactly calculate the effect of decoherence and the finite range of interactions on the maximum spin squeezing achievable in experiment. Figure 4 shows the expected maximal squeezing and antisqueezing as a function of angle ψ in the yz plane for $\zeta = 0, 3$, with $\Gamma = 0.06J$ and $\Gamma_{el} = 8\Gamma_{ud} = 8\Gamma_{du}$ (typical experimental numbers in [10]). The effects of decoherence are more pronounced for shorter-range interactions due to the longer time scales for maximal squeezing. For this calculation the spins are assumed to be initialized (prior to the Ising dynamics) in a coherent state pointing along the x axis, and we define the spin-squeezing parameter,

$$\xi(\psi) = \frac{\sqrt{\mathcal{N}} \Delta S^\psi}{\langle \hat{S}^x \rangle}, \quad (14)$$

with $\Delta A = \sqrt{\langle \hat{A}^2 \rangle - \langle \hat{A} \rangle^2}$, $\hat{S}^\psi = \frac{1}{2} \sum_j \hat{\sigma}_j^\psi$, and $\hat{\sigma}_j^\psi = \cos(\psi) \hat{\sigma}_j^y + \sin(\psi) \hat{\sigma}_j^z$. Notably, in the long-ranged interaction limit [39] the spin squeezing is degraded but still quite appreciable under *current* experimental conditions (for short-range interactions, $\zeta = 3$, the spin squeezing is completely destroyed by decoherence).

For the current experimental parameters there is essentially no spin revival, and no indication of a MSS at $\tau_r/2$. However, assuming 97 ions and expected improvements in the experiment [10] (a roughly 50-fold increase in the ratio J/Γ), in Fig. 5 we show that transverse-spin revivals begin to appear. In that figure, the dotted line is obtained by treating the decoherence at the single-particle level, which amounts to attaching a decaying exponential $e^{-\Gamma t}$ to the operators $\hat{\sigma}^x$ and $\hat{\sigma}^y$. We note that this treatment would be exact if the decoherence were only of the Rayleigh type ($\Gamma_r = 0$). The solid line is the full solution from Eq. (10); the large (~ 35 -fold) discrepancy between the single-particle and exact results indicates that a proper accounting of Raman decoherence

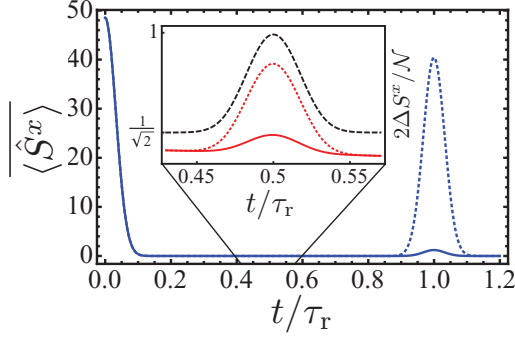


FIG. 5. (Color online) Transverse-spin relaxation and revivals for $\zeta = 0$, with parameters corresponding to expected experimental capabilities in [10] (blue solid line). The dotted blue line is obtained by treating decoherence at the single-particle level, and underestimates the detrimental effect of Raman decoherence by about a factor of 35. Inset: transverse-spin fluctuations peaking at time $\tau_r/2$. Experimental parameters, exact treatment (red solid line); experimental parameters, single-particle treatment (red-dotted line); no decoherence (black dashed line).

processes, which is achieved in our solution, will be essential for understanding the behavior of this experiment. In the inset of Fig. 5 we plot the transverse-spin fluctuations ΔS^x at times near $\tau_r/2$. The peak in these fluctuations (which would achieve unity in the absence of decoherence) is a result of strong transverse-spin correlations in an emerging MSS, indicating that the expected improvements to the experiments will bring within reach the production of MSS's of ~ 100 ions in the near future.

VI. CONCLUSIONS

These calculations provide a rare glimpse into the exact structure of relaxation dynamics in an open and strongly interacting quantum system. The surprisingly large detrimental effect of Raman decoherence—which far exceeds that expected from a single-particle picture—is the result of an interaction-mediated back action of decohered spins on the remaining many-body system, in which each Raman-flipped spin behaves as a (temporally) fluctuating magnetic field. Interestingly, our exact solution reveals that the net effect of this back action is (for $\zeta = 0$) a global rotation in spin space, which in principle can be corrected if the arrival times of spontaneously scattered photons are recorded. These ideas will be explored in more detail in future work.

Note added. Recently, we were informed of simultaneous calculation of spin-spin correlation functions for quantum Ising models in the absence of decoherence [40].

ACKNOWLEDGMENTS

We gratefully acknowledge Joe Britton, Brian Sawyer, Salvatore Manmana, Michael Kastner, Dominic Meiser, and Murray Holland for helpful discussions. This work was supported by NIST, the NSF (PIF and PFC grants), AFOSR and ARO individual investigator awards, and the ARO with funding from the DARPA-OLE program. K.H. thanks the NRC for support. This manuscript is the contribution of NIST and is not subject to US copyright.

APPENDIX A: EXPRESSIONS FOR SPIN LENGTH AND CORRELATION FUNCTIONS ALONG A SINGLE TRAJECTORY

As in the main text, we write the state of a single spin as $\sum_{\sigma_j^z} f_j(\sigma_j^z) |\sigma_j^z\rangle$, where σ_j^z is an index that takes on the eigenvalues of the operator $\hat{\sigma}_j^z$, $f_j(1) = \cos(\theta_j/2)e^{i\varphi_j/2}$, and $f_j(-1) = \sin(\theta_j/2)e^{-i\varphi_j/2}$. The initial state of the entire system is taken to be a direct product of states for each individual spin:

$$\begin{aligned} |\psi(0)\rangle &\equiv \bigotimes_j \sum_{\sigma_j} f_j(\sigma_j) |\sigma_j\rangle \\ &= \sum_{\sigma_1^z, \dots, \sigma_N^z} f_1(\sigma_1^z) \times \dots \times f_N(\sigma_N^z) |\sigma_1^z, \dots, \sigma_N^z\rangle. \end{aligned} \quad (\text{A1})$$

As discussed in the main text, evaluating all of the Rayleigh jumps at $t = 0$ can be accomplished by changing $\varphi_j \rightarrow \varphi_j + \pi \mathcal{F}_j$, which rotates the spin on site j by an angle π if it has undergone an odd number of Rayleigh jumps. Raman jumps can be incorporated at $t = 0$ by setting $\theta_j = 0(\pi)$ if the final Raman jump on site j was $\hat{\sigma}_j^+$ ($\hat{\sigma}_j^-$). We therefore define $\tilde{f}_j(\sigma_j^z)$ to be the modification of $f_j(\sigma_j^z)$ under those transformations. We also note that spins having undergone one or more Raman jumps are treated as an effective magnetic field, and not included in the spin-spin coupling term of the Hamiltonian. This is accomplished by changing $J_{ij} \rightarrow \alpha_i \alpha_j J_{ij}$ (with $\alpha_j = \delta_{\mathcal{R}_j, 0}$) in the Hamiltonian and including an effective magnetic field. Therefore, we can write the (time-dependent) wave function $|\tilde{\psi}(t)\rangle$ evolving under \mathcal{U} [as defined in Eq. (6) of the manuscript] as

$$|\tilde{\psi}(t)\rangle = \sum_{\sigma_1^z, \dots, \sigma_N^z} \exp \left[-it \left(\frac{1}{N} \sum_{i,j} \alpha_i \alpha_j J_{ij} \sigma_i^z \sigma_j^z + \sum_j (\eta_j - i\gamma) \sigma_j^z \right) \right] \tilde{f}_1(\sigma_1^z) \times \dots \times \tilde{f}_N(\sigma_N^z) |\sigma_1^z, \dots, \sigma_N^z\rangle. \quad (\text{A2})$$

In order to calculate the transverse-spin length we will first calculate $\langle \hat{\sigma}_j^+ \rangle = \langle \tilde{\psi}(t) | \hat{\sigma}_j^+ | \tilde{\psi}(t) \rangle / \langle \tilde{\psi}(t) | \tilde{\psi}(t) \rangle$, and at the end obtain $\langle \hat{S}^x \rangle = \text{Re}(\sum_j \langle \hat{\sigma}_j^+ \rangle)$.

Let's imagine, in particular, calculating $\langle \tilde{\psi}(t) | \hat{\sigma}_1^+ | \tilde{\psi}(t) \rangle$ (there is nothing special about the first spin; this just makes the notation in what follows less confusing). Because the wave function enters twice, this would involve two sums like the one in Eq. (A2), over σ_j^z and $\sigma_j'^z$, but very few terms survive: we need $\sigma_1^z = -1$, $\sigma_1'^z = 1$, and for all $j \neq 1$ we must have $\sigma_j^z = \sigma_j'^z$, so the matrix

element is given by

$$\langle \tilde{\psi}(t) | \hat{\sigma}_1^+ | \tilde{\psi}(t) \rangle = \tilde{f}_1^*(1) \tilde{f}_1(-1) \sum_{\sigma_2^z, \dots, \sigma_N^z} |\tilde{f}_2(\sigma_2^z)|^2 \times \dots \times |\tilde{f}_N(\sigma_N^z)|^2 \exp \left[2it \left(\eta_1 + \sum_{j=2}^N \frac{1}{N} \alpha_1 \alpha_j J_{1j} \sigma_j^z + i \alpha_j \gamma \sigma_j^z \right) \right]. \quad (\text{A3})$$

If $\alpha_j = 0$, the j th spin always has a well-defined value of σ_j^z and the choice to include the term $\gamma \sigma_j^z$ in the exponentiated sum (or not) only affects the overall normalization of the wave function. By multiplying γ by α_j (in the exponentiated sum), we have chosen to not include the term $\gamma \sigma_j^z$, and this is properly accounted for when normalizing this expectation value below. In order to obtain $\langle \hat{\sigma}_1^+ \rangle$ we must divide by the (nonconserved) normalization of the wave function $\langle \tilde{\psi}(t) | \tilde{\psi}(t) \rangle$. Defining $g_j(x) = \sum_{\sigma} |f_j(\sigma)|^2 e^{-\sigma x}$ (as in the manuscript), we obtain

$$\langle \hat{\sigma}_1^+ \rangle = \frac{\tilde{f}_1^*(1) \tilde{f}_1(-1)}{g_1(2\gamma t)} \sum_{\sigma_2^z, \dots, \sigma_N^z} \frac{|\tilde{f}_2(\sigma_2^z)|^2}{g_2(2\alpha_2 \gamma t)} \times \dots \times \frac{|\tilde{f}_N(\sigma_N^z)|^2}{g_N(2\alpha_N \gamma t)} \exp \left[2it \left(\eta_1 + \sum_{j=2}^N \frac{1}{N} \alpha_1 \alpha_j J_{1j} \sigma_j^z + i \alpha_j \gamma \sigma_j^z \right) \right]. \quad (\text{A4})$$

This expression can be simplified by making the following set of observations: (1) $\tilde{f}_1^*(1) \tilde{f}_1(-1) = \alpha_1 \beta_1 e^{i\varphi_1} \sin(\theta_1)/2$ [as in the text, $\beta_j = (-1)^{\mathcal{F}_j}$], (2) the α_1 in the exponent is irrelevant, because if it takes the value 0 the entire expression for $\langle \tilde{\psi}(t) | \hat{\sigma}_1^+ | \tilde{\psi}(t) \rangle$ vanishes, and (3) the summand factorizes into a product where each term contains only local (i.e., on a single site) variables, and hence the sum of products can be exchanged for a product of sums. Taking observations (1)–(3) into account, we obtain

$$\langle \hat{\sigma}_1^+ \rangle = \frac{\sin(\theta_1) e^{i\varphi_1}}{2g_1(2\gamma t)} \alpha_1 \beta_1 \prod_{j=2}^N \left(\sum_{\sigma_j^z} \frac{|\tilde{f}_j(\sigma_j^z)|^2}{g_j(2\alpha_j \gamma t)} \exp[2it \alpha_j \sigma_j^z (J_{1j}/N + i\gamma)] e^{2i J_{1j} \tau_j / N} \right) \quad (\text{A5a})$$

$$= \frac{\sin(\theta_1) e^{i\varphi_1}}{2g_1(2\gamma t)} \alpha_1 \beta_1 \prod_{j=2}^N \left(e^{2i J_{1j} \tau_j / N} \frac{g_j[2\alpha_j t(\gamma - i J_{1j}/N)]}{g_j(2\gamma t \alpha_j)} \right). \quad (\text{A5b})$$

Therefore, we can write

$$\langle \hat{S}^x \rangle = \text{Re} \sum_{j=1}^N \left[\frac{\sin(\theta_j) e^{i\varphi_j}}{2g_j(2\gamma t)} \alpha_j \beta_j \prod_{k \neq j} \left(e^{2i J_{jk} \tau_k / N} \frac{g_k[2\alpha_k t(\gamma - i J_{jk}/N)]}{g_k(2\gamma t \alpha_k)} \right) \right]. \quad (\text{A6})$$

The calculation of correlation functions follows from extremely similar considerations. For instance, let's consider $\mathcal{G}_{jk}^{++} \equiv \langle \hat{\sigma}_j^- \hat{\sigma}_k^+ \rangle$. In this case, the operators in the expectation value only connect two states if $-\sigma_j^z = \sigma_k^z = 1$, $\sigma_k^z = -\sigma_k^z = 1$, and $\sigma_l^z = \sigma_l^z$ whenever $l \notin \{j, k\}$. Therefore, much as before we have

$$\mathcal{G}_{jk}^{++} = \frac{\sin(\theta_j) \sin(\theta_k) e^{i(\varphi_k - \varphi_j)}}{4g_j(2\gamma t) g_k(2\gamma t)} \alpha_j \alpha_k \beta_j \beta_k \prod_{l \notin \{j, k\}} \left(e^{2i(J_{kl} - J_{jl})\tau_l / N} \frac{g_l[2\alpha_l t(\gamma - i[J_{kl} - J_{jl}]/N)]}{g_l(2\gamma t \alpha_l)} \right). \quad (\text{A7})$$

Computing correlation functions involving a single $\hat{\sigma}^z$, such as $\mathcal{G}_{jk}^{z+} \equiv \langle \hat{\sigma}_j^z \hat{\sigma}_k^+ \rangle$, can be achieved by inserting σ_j^z into the sum in Eq. (A4), yielding

$$\mathcal{G}_{jk}^{z+} = \frac{\sin(\theta_k) e^{i\varphi_k} \alpha_k \beta_k}{2g_k(2\gamma t)} \left[\alpha_j \frac{\cos^2(\theta/2) e^{-2\gamma t} - \sin^2(\theta/2) e^{2\gamma t}}{g_j(2\gamma t)} + (1 - \alpha_j) \kappa_j \right] \prod_{l \notin \{j, k\}} \left(e^{2i J_{kl} \tau_l / N} \frac{g_l[2\alpha_l t(\gamma - i J_{kl}/N)]}{g_l(2\gamma t \alpha_l)} \right). \quad (\text{A8})$$

Assuming one or more Raman flip occurred, the variable κ_j takes on the values ± 1 if the final Raman jump is $\hat{\sigma}_j^{\pm}$.

APPENDIX B: ANALYTIC EVALUATION OF STOCHASTIC AVERAGING OF TRAJECTORIES

At this point in the calculation, for clarity of presentation, we set $\varphi_j = 0$ and $\theta_j = \pi/2$ (for all j), so all spins point along the x axis at $t = 0$. Defining $\mathcal{P}(\mathcal{R}, \mathcal{F}, \tau)$ to be the probability distribution of the variables \mathcal{R} , \mathcal{F} , and τ on a single site (it is

the same on every site), the trajectory averaged expectation value is given by

$$\overline{\langle \hat{\sigma}_j^+ \rangle} = \sum_{\text{all } \mathcal{R}} \sum_{\text{all } \mathcal{F}} \int d\tau_1 \dots \int d\tau_N \langle \hat{\sigma}_j^+ \rangle \prod_k \mathcal{P}(\mathcal{R}_k, \mathcal{F}_k, \tau_k). \quad (\text{B1})$$

To begin, we note that the probability distribution can be decomposed as $\mathcal{P}(\mathcal{R}, \mathcal{F}, \tau) = \mathcal{P}_{\text{el}}(\mathcal{F})\mathcal{P}_r(\mathcal{R}, \tau)$, which is valid because the probability of Rayleigh jump is independent of whether a Raman jump has occurred (and vice versa). The occurrence of random processes follows a Poissonian distribution, so $\mathcal{P}_{\text{el}}(\mathcal{F}) = e^{-\Gamma_{\text{el}}t/4}(\Gamma_{\text{el}}t/4)^{\mathcal{F}}/\mathcal{F}!$, and we have also calculated \mathcal{P}_r . The result depends on whether \mathcal{R} is even or odd (the proof is simple but requires some careful reasoning, and we do not give it here). We parametrize the \mathcal{R} -odd solution by $\mu = (\mathcal{R} - 1)/2$ (which will run over all non-negative integers), and we parametrize the \mathcal{R} -even solutions by $\mu = (\mathcal{R} - 2)/2$ (once again running μ over all

non-negative integers), and obtain

$$\begin{aligned}\mathcal{P}_r^{\text{odd}}(\mu, \tau) &= \frac{\Gamma_r}{4} e^{-\Gamma_r t/2} \frac{(\Gamma_{\text{ud}}\Gamma_{\text{du}}/4)^{\mu}}{(\mu!)^2} e^{-2\tau\gamma} (t^2 - \tau^2)^{\mu}, \\ \mathcal{P}_r^{\text{even}}(\mu, \tau) &= \frac{\Gamma_{\text{ud}}\Gamma_{\text{du}}t}{4} e^{-\Gamma_r t/2} \frac{(\Gamma_{\text{ud}}\Gamma_{\text{du}}/4)^{\mu}}{\mu!(\mu+1)!} e^{-2\tau\gamma} (t^2 - \tau^2)^{\mu}.\end{aligned}\quad (\text{B2})$$

By evaluating the sum

$$\sum_{\mathcal{F}=0}^{\infty} \mathcal{P}_{\text{el}}(\mathcal{F}) e^{i\pi\mathcal{F}} = e^{-\Gamma_{\text{el}}t/2}, \quad (\text{B3})$$

we obtain

$$\begin{aligned}\overline{\langle \hat{\sigma}_j^+ \rangle} &= \frac{e^{-\Gamma_{\text{el}}t/2}}{2 \cosh(2\gamma t)} \sum_{\mathcal{R}_1, \dots, \mathcal{R}_N} \int d\tau_1 \dots \int d\tau_N \left[\mathcal{P}(\mathcal{R}_j, \tau_j) \alpha_j \prod_{k \neq j} e^{2iJ_{jk}\tau_k/\mathcal{N}} \frac{\cosh[2\alpha_k t(\gamma - iJ_{jk}/\mathcal{N})]}{\cosh(2\gamma t\alpha_k)} \mathcal{P}_r(\mathcal{R}_k, \tau_k) \right] \\ &= \frac{e^{-\Gamma_{\text{el}}t/2}}{2 \cosh(2\gamma t)} \left[\sum_{\mathcal{R}_j} \int d\tau_j \alpha_j \mathcal{P}(\mathcal{R}_j, \tau_j) \right] \left[\prod_{j \neq k} \sum_{\mathcal{R}_k} \int d\tau_k e^{2iJ_{jk}\tau_k/\mathcal{N}} \frac{\cosh[2\alpha_k t(\gamma - iJ_{jk}/\mathcal{N})]}{\cosh(2\gamma t\alpha_k)} \mathcal{P}_r(\mathcal{R}_k, \tau_k) \right].\end{aligned}$$

Because α_j gives 1 if there have not been any Raman flips at site j and 0 otherwise, the term in the first square bracket is just the probability that there has been no Raman flip on site j , which is given by $e^{-\Gamma_r t/2} \cosh(2\gamma t)$ [this comes from evolving the wave function of a single spin pointing along x with the effective Hamiltonian Eq. (4)]. Therefore, we have

$$\overline{\langle \hat{\sigma}_j^+ \rangle} = \frac{1}{2} e^{-\Gamma t} \left[\prod_{j \neq k} \sum_{\mathcal{R}_k} \int d\tau_k e^{2iJ_{jk}\tau_k/\mathcal{N}} \frac{\cosh[2\alpha_k t(\gamma - iJ_{jk}/\mathcal{N})]}{\cosh(2\gamma t\alpha_k)} \mathcal{P}_r(\mathcal{R}_k, \tau_k) \right]. \quad (\text{B4})$$

Defining $s = 2i\gamma + 2J/\mathcal{N}$, the trick is now to evaluate the quantity

$$\begin{aligned}\Phi(J, t) &= \sum_{\mathcal{R}} \int d\tau \mathcal{P}(\mathcal{R}, \tau) e^{2iJ\tau/\mathcal{N}} \frac{\cosh(ist\alpha)}{\cosh(2\gamma t\alpha)} \\ &= e^{-\Gamma_r t/2} \cosh(ist) + \sum_{\mathcal{R}=1}^{\infty} \int d\tau \mathcal{P}(\mathcal{R}, \tau) e^{2iJ\tau/\mathcal{N}}.\end{aligned}\quad (\text{B5})$$

The second equality follows from pulling off the $\mathcal{R} = 0$ term in the sum, which represents the probability of having no Raman flip (and so we can set $\tau = 0$ and $\alpha = 1$ in this term). The second term represents the probability for any finite number of Raman flips, and hence we must keep τ arbitrary but can set $\alpha = 0$. The integral over τ can be evaluated by using the identity

$$\int_{-t}^t d\tau (t^2 - \tau^2)^{\mu} e^{-ix\tau} = (2t)^{\mu+1} \frac{j_{\mu}(xt)\mu!}{(x)^{\mu}}, \quad (\text{B6})$$

where j is a spherical Bessel function. The remaining sum over \mathcal{R} can be recognized as a generating function for the

spherical Bessel functions (or a derivative thereof). Defining parameters $\lambda = \Gamma_r/2$ and $r = \Gamma_{\text{ud}}\Gamma_{\text{du}}$, and functions

$$F(x, y) = \text{sinc}(\sqrt{x^2 - y}), \quad (\text{B7})$$

$$G(x, y) = \frac{\cos(\sqrt{x^2 - y}) - \cos(x)}{x}, \quad (\text{B8})$$

we obtain

$$\begin{aligned}\Phi(J, t) &= e^{-\lambda t} \cos(st) + \lambda t e^{-\lambda t} F(st, rt) + st e^{-\lambda t} G(st, rt) \\ &= e^{-\lambda t} [\cos(t\sqrt{s^2 - r}) + \lambda t \text{sinc}(t\sqrt{s^2 - r})].\end{aligned}\quad (\text{B9})$$

We can now write out the exact solution,

$$\overline{\langle \hat{S}^x \rangle} = \frac{e^{-\Gamma t}}{2} \text{Re} \sum_j \prod_{k \neq j} \Phi(J_{jk}, t). \quad (\text{B10})$$

Because Eqs. (A6) and (A7) have such a similar structure, the stochastic averaging of correlation functions is almost identical, and leads to the similar expressions given in the main text [Eqs. (10) and (11)].

- [1] S. Diehl, E. Rico, M. Baranov, and P. Zoller, *Nature Phys.* **7**, 971 (2011).
[2] E. Dalla Torre, E. Demler, T. Giamarchi, and E. Altman, *Nature Phys.* **6**, 802 (2010).

- [3] T. E. Lee, H. Häffner, and M. C. Cross, *Phys. Rev. Lett.* **108**, 023602 (2012).
[4] B. Kraus, H. P. Büchler, S. Diehl, A. Kantian, A. Micheli, and P. Zoller, *Phys. Rev. A* **78**, 042307 (2008).

- [5] S. Diehl, A. Micheli, A. Kantian, B. Kraus, H. P. Büchler, and P. Zoller, *Nature Phys.* **4**, 878 (2008).
- [6] M. Foss-Feig, A. J. Daley, J. K. Thompson, and A. M. Rey, *Phys. Rev. Lett.* **109**, 230501 (2012).
- [7] I. Bloch, J. Dalibard, and W. Zwerger, *Rev. Mod. Phys.* **80**, 885 (2008).
- [8] R. Horodecki, P. Horodecki, M. Horodecki, and K. Horodecki, *Rev. Mod. Phys.* **81**, 865 (2009).
- [9] V. Giovannetti, S. Lloyd, and L. Maccone, *Nat. Photonics* **5**, 222 (2011).
- [10] J. W. Britton, B. C. Sawyer, A. C. Keith, C.-C. J. Wang, J. K. Freericks, H. Uys, M. J. Biercuk, and J. J. Bollinger, *Nature (London)* **484**, 489 (2012).
- [11] K. Kim, M.-S. Chang, S. Korenblit, R. Islam, E. Edwards, J. Freericks, G.-D. Lin, L.-M. Duan, and C. Monroe, *Nature (London)* **465**, 590 (2010).
- [12] R. Islam, E. Edwards, K. Kim, S. Korenblit, C. Noh, H. Carmichael, G.-D. Lin, L.-M. Duan, C.-C. Joseph Wang, J. Freericks *et al.*, *Nat. Commun.* **2**, 377 (2011).
- [13] K.-K. Ni, S. Ospelkaus, M. H. G. de Miranda, A. Pe'er, B. Neyenhuis, J. J. Zirbel, S. Kotochigova, P. S. Julienne, D. S. Jin, and J. Ye, *Science* **322**, 231 (2008).
- [14] A. V. Gorshkov, S. R. Manmana, G. Chen, J. Ye, E. Demler, M. D. Lukin, and A. M. Rey, *Phys. Rev. Lett.* **107**, 115301 (2011).
- [15] H. Weimer, M. Müller, I. Lesanovsky, P. Zoller, and H. P. Büchler, *Nature Phys.* **6**, 382 (2010).
- [16] R. Löw, H. Weimer, U. Krohn, R. Heidemann, V. Bendkowsky, B. Butscher, H. P. Büchler, and T. Pfau, *Phys. Rev. A* **80**, 033422 (2009).
- [17] S. Gopalakrishnan, B. L. Lev, and P. M. Goldbart, *Phys. Rev. Lett.* **107**, 277201 (2011).
- [18] P. Strack and S. Sachdev, *Phys. Rev. Lett.* **107**, 277202 (2011).
- [19] M. D. Swallows, M. Bishof, Y. Lin, S. Blatt, M. J. Martin, A. M. Rey, and J. Ye, *Science* **331**, 1043 (2011).
- [20] I. Chiorescu, Y. Nakamura, C. J. P. M. Harmans, and J. E. Mooij, *Science* **299**, 1869 (2003).
- [21] R. Hanson, L. P. Kouwenhoven, J. R. Petta, S. Tarucha, and L. M. K. Vandersypen, *Rev. Mod. Phys.* **79**, 1217 (2007).
- [22] S. Praver and A. D. Greentree, *Science* **320**, 1601 (2008).
- [23] M. Kitagawa and M. Ueda, *Phys. Rev. A* **47**, 5138 (1993).
- [24] A. Sorensen, L.-M. Duan, J. I. Cirac, and P. Zoller, *Nature (London)* **409**, 63 (2001).
- [25] C. Gross *et al.*, *Nature (London)* **464**, 1165 (2010).
- [26] K. Mølmer and A. Sørensen, *Phys. Rev. Lett.* **82**, 1835 (1999).
- [27] T. Monz, P. Schindler, J. T. Barreiro, M. Chwalla, D. Nigg, W. A. Coish, M. Harlander, W. Hänsel, M. Hennrich, and R. Blatt, *Phys. Rev. Lett.* **106**, 130506 (2011).
- [28] D. Leibfried, E. Knill, S. Seidelin, J. Britton, R. B. Blakestad, J. Chiaverini, D. B. Hume, W. M. Itano, J. D. Jost, C. Langer *et al.*, *Nature (London)* **438**, 639 (2005).
- [29] R. Raussendorf and H. J. Briegel, *Phys. Rev. Lett.* **86**, 5188 (2001).
- [30] This master equation could be slightly generalized by allowing the decoherence rates to vary from site to site. This can be taken into account trivially by adding site indices to these rates in the final expressions, Eqs. (10)–(12).
- [31] M. B. Plenio and P. L. Knight, *Rev. Mod. Phys.* **70**, 101 (1998).
- [32] H. Uys, M. J. Biercuk, A. P. VanDevender, C. Ospelkaus, D. Meiser, R. Ozeri, and J. J. Bollinger, *Phys. Rev. Lett.* **105**, 200401 (2010).
- [33] G. G. Emch, *J. Math. Phys.* **7**, 1198 (1966).
- [34] C. Radin, *J. Math. Phys.* **11**, 2945 (1970).
- [35] M. Kastner, *Phys. Rev. Lett.* **106**, 130601 (2011).
- [36] K. R. A. Hazzard, S. Manmana, M. Foss-Feig, and A. M. Rey, *Phys. Rev. Lett.* **110**, 075301 (2013).
- [37] K. R. A. Hazzard, S. Manmana, M. Foss-Feig, and A. M. Rey (in preparation).
- [38] Despite superficial appearances, notice that $\Phi(0,t) = 1$ (and not $e^{-\Gamma t/2}$), justifying the designation of Γ as the total decay rate, as in [32].
- [39] In Ref. [10], $\alpha \lesssim 0.1$ is possible.
- [40] M. van den Worm, R. Paskauskas, B. Sawyer, J. Bollinger, and M. Kastner, arXiv:1209.3697.